HHS Public Access

Author manuscript

J Nucl Med. Author manuscript; available in PMC 2015 July 14.

Published in final edited form as:

J Nucl Med. 2015 January ; 56(1): 76–81. doi:10.2967/jnumed.114.146381.

Imaging Pulmonary Inducible Nitric Oxide Synthase Expression with PET

Howard J. Huang[1], **Warren Isakow**[1], **Derek E. Byers**[1], **Jacquelyn T. Engle**[2], **Elizabeth A. Griffin**[2], **Debra Kemp**[3], **Steven L. Brody**[1,2], **Robert J. Gropler**[2], **J. Philip Miller**[4], **Wenhua Chu**[2], **Dong Zhou**[2], **Richard A. Pierce**[1], **Mario Castro**[1], **Robert H. Mach**[2], and **Delphine L. Chen**[1,2]

[1]Division of Pulmonary and Critical Care Medicine, Department of Internal Medicine, Washington University School of Medicine, St. Louis, Missouri

[2]Mallinckrodt Institute of Radiology, Washington University School of Medicine, St. Louis, Missouri

[3]Center for Clinical Studies, Department of Internal Medicine, Washington University School of Medicine, St. Louis, Missouri

[4]Division of Biostatistics, Washington University School of Medicine, St. Louis, Missouri

Abstract

Inducible nitric oxide synthase (iNOS) activity increases in acute and chronic inflammatory lung diseases. Imaging iNOS expression may be useful as an inflammation biomarker for monitoring lung disease activity. We developed a novel tracer for PET that binds to iNOS in vivo, ^{18}F-NOS. In this study, we tested whether ^{18}F-NOS could quantify iNOS expression from endotoxin-induced lung inflammation in healthy volunteers.

Methods—Healthy volunteers were screened to exclude cardiopulmonary disease. Qualifying volunteers underwent a baseline, 1-h dynamic ^{18}F-NOS PET/CT scan. Endotoxin (4 ng/kg) was then instilled bronchoscopically in the right middle lobe. ^{18}F-NOS imaging was performed again approximately 16 h after endotoxin instillation. Radiolabeled metabolites were determined from blood samples. Cells recovered by bronchoalveolar lavage (BAL) after imaging were stained immunohistochemically for iNOS. ^{18}F-NOS uptake was quantified as the distribution volume ratio (DVR) determined by Logan plot graphical analysis in volumes of interest placed over the area of endotoxin instillation and in an equivalent lung region on the left. The mean Hounsfield units (HUs) were also computed using the same volumes of interest to measure density changes.

For correspondence contact: Delphine L. Chen, Divisions of Radiological Sciences and Nuclear Medicine, Mallinckrodt Institute of Radiology, Washington University School of Medicine, Campus Box 8225, 510 S. Kingshighway Blvd., St. Louis, MO 63110. chend@mir.wustl.edu.

DISCLOSURE

This study was funded by the Barnes-Jewish Hospital Foundation and K08 EB006702, R01 HL116389, R01 HL121218, NIH/K08 HL107677, and a Doris Duke Charitable Foundation Clinical Investigator Award. The Washington University Institute for Clinical and Translational Sciences grant UL1 TR000448 from the National Center for Advancing Translational Sciences of the NIH also supported volunteer recruitment through the Recruitment Enhancement Core. This trial's clinicaltrials.gov record number is NCT01407796. No other potential conflict of interest relevant to this article was reported. The content is solely the responsibility of the authors and does not necessarily represent the official view of the NIH.

Results—Seven healthy volunteers with normal pulmonary function completed the study with evaluable data. The DVR increased by approximately 30%, from a baseline mean of 0.42 ± 0.07 to 0.54 ± 0.12, and the mean HUs by 11% after endotoxin in 6 volunteers who had positive iNOS staining in BAL cells. The DVR did not change in the left lung after endotoxin. In 1 volunteer with low-level iNOS staining in BAL cells, the mean HUs increased by 7% without an increase in DVR. Metabolism was rapid, with approximately 50% of the parent compound at 5 min and 17% at 60 min after injection.

Conclusion—^{18}F-NOS can be used to image iNOS activity in acute lung inflammation in humans and may be a useful PET tracer for imaging iNOS expression in inflammatory lung disease.

Keywords

endotoxin; inducible nitric oxide synthase; lung inflammation; positron emission tomography

Inflammation contributes to many acute and chronic lung diseases. These diseases are associated with high morbidity and mortality rates as well as significant health-care use (1–3). Despite this socioeconomic burden, therapeutic development for respiratory indications lags that of other disease areas (4). This deficiency has been attributed in part to the lack of reliable biomarkers that accurately localize and quantify lung disease activity and assess response to treatment (5).

Currently available techniques for assessing lung inflammation include invasive methods such as bronchoalveolar lavage (BAL) and lung tissue biopsy to directly examine immune cells. Induced sputum, although minimally invasive, requires significant patient effort to obtain adequate samples and is difficult to reproduce. Moreover, these tissue-based methods do not provide a global assessment of the inflammatory disease burden or information regarding cellular activity or function. Thus, noninvasive, molecular-based techniques for quantifying inflammation could improve on or provide complementary information to these existing approaches.

Several imaging methods have been investigated as potential noninvasive biomarkers for lung inflammation. CT can provide more detailed lung parenchymal characterization for inflammation than plain radiographs (6), but the signal is nonspecific as infiltrates and thickening of the airways can be due to noninflammatory processes, such as edema or hemorrhage. ^{18}F-FDG imaging with PET has been used to measure neutrophilic lung inflammation in patients with acute respiratory distress syndrome, cystic fibrosis, and chronic obstructive pulmonary disease (7–10). However, neoplastic and fibrotic processes also increase glucose utilization, thus decreasing the specificity of ^{18}F-FDG for inflammation. Therefore, there remains a need for novel PET tracers that detect the expression of specific inflammatory markers in lung tissue.

Inducible nitric oxide synthase (iNOS, NOS2) is 1 of 3 nitric oxide synthase (NOS) isoforms that is constitutively expressed in normal lung epithelium (11) and is also induced by inflammatory stimuli (12). Increased iNOS has been associated with either disease severity or progression in asthma (13,14), chronic obstructive pulmonary disease (15–17), and acute

respiratory distress syndrome (18,19). Preclinical studies also suggest a mechanistic link between iNOS expression and the development of emphysema, pulmonary hypertension, and asthma (20,21). Thus, noninvasive methods for imaging iNOS expression may be useful as a more specific biomarker of inflammatory lung disease activity. We have developed a PET tracer, ^{18}F-NOS, that binds to iNOS (22) and has been used to image iNOS expression in heart transplant recipients (23). To assess its potential utility for imaging lung-related inflammation, we hypothesized that ^{18}F-NOS could image iNOS expression in human lungs after endotoxin instillation.

MATERIALS AND METHODS

Study Design and Procedure Flow

This study was approved by the Institutional Review Board and conducted in compliance with the Health Insurance Portability and Accountability Act under Investigational New Drug (IND) #100042 for endotoxin and exploratory IND #106089 for ^{18}F-NOS. All volunteers signed a written informed consent form. Eligible volunteers had no cardiopulmonary disease and normal spirometry, chest radiographs, electrocardiograms, and screening blood evaluations. Detailed eligibility criteria are listed in the supplemental materials (available at http://jnm.snmjournals.org).

Figure 1 illustrates the study procedure flow. Eligible volunteers underwent a baseline ^{18}F-NOS PET/CT scan in the morning, followed by endotoxin instillation. A postendotoxin ^{18}F-NOS PET/CT scan was obtained the following morning, approximately 16 h later, followed by BAL. Spirometry testing was repeated after endotoxin administration. ^{18}F-NOS was synthesized as previously described (23). Vital sign monitoring was performed throughout the study as previously reported (24).

Endotoxin Instillation and BAL

Bronchoscopic endotoxin instillation (4 ng/kg in 2 mL of sterile water) and BAL were performed as previously described (24,25). The supplemental materials provide details. For BAL, 3 sequential 50-mL volumes of warmed sterile saline (37°C) were instilled in the suction channel of the bronchoscope, recovered by gentle aspiration, and pooled for analysis.

BAL Cell Processing and Immunohistochemical Staining

Cytospins of 3×10^5 BAL cells were created on slides, air-dried and fixed in 100% methanol, and stored at 4°C until ready for staining. One slide was stained with Hema 3 (#123-869; Fisher Scientific) to determine the percentage of macrophages and neutrophils. Slides were stained with 1 of 2 different polyclonal rabbit antihuman iNOS antibodies for fluorescence microscopy (#AB5384 that binds at the C terminus, 1:200 dilution [Millipore], or #SC-8310, clone H-174, that binds the N terminus, 1:50 dilution [Santa Cruz]) so that each volunteer had at least 1 slide stained with each iNOS antibody (at least 2 slides total stained). The supplemental materials provide details.

Exhaled Nitric Oxide Measurement

Exhaled nitric oxide measurements were obtained as previously described (26) using a NIOX MINO (Aerocrine). The baseline measurements were obtained independently before spirometry. The post-endotoxin measurements were collected before spirometry on the same day. The fractional exhaled nitric oxide (FeNO) was reported as parts per billion (ppb).

Single Nucleotide Polymorphism (SNP) Testing

Toll-like receptor 4 (TLR4) polymorphisms Asp299Gly (rs4986790) and Thr399Ile (rs4986791), associated with decreased endotoxin responsiveness, were tested in all volunteers (27). DNA was extracted from whole blood using the PureGene protocol (Qiagen) according to the manufacturer's instructions and sent for genotyping by DNA Genotek, Inc. (Kanata, Ontario).

Image Acquisition

Scans were obtained on a Siemens Biograph 40 PET/CT scanner. After a low-dose attenuation-correction CT scan (tube current, 80 mA; pitch, 0.8; collimation, 28.8 mm; effective mAs, 50) was obtained, a 1-h PET dynamic acquisition was started at the time of a bolus intravenous injection of ^{18}F-NOS (267 ± 6.5 MBq [7.2 ± 0.2 mCi], 0.35 ± 0.16 μg of total mass) with the following framing schedule: 24 × 5 s, 6 × 3 min, and 7 × 5 min frames. Venous blood samples were obtained according to the following schedule: 4 × 30 s, 4 × 1 min, 2 × 2.5 min, 2 × 5 min, and 10 × 10 min. The attenuation-correction CT images were reconstructed with 3-mm slices using a B19f kernel. PET images were reconstructed using filtered backprojection (gaussian filter, 5 mm).

Image Analysis

The DICOM PET and CT image files were imported into Integrated Research Workflow 4.0 (Siemens) for analysis. The preendotoxin PET and CT images were aligned to the coregistered postendotoxin PET and CT images. Volumes of interest (VOIs) were placed on the areas of infiltrate in the right middle lobe and in an equivalent region of lung on the left using standard lung windows (center, −500 Hounsfield units [HUs]; width, 1,500 HU). The time–activity curves were then extracted from these VOIs on both the baseline and the postendotoxin ^{18}F-NOS PET scans. A VOI over the main pulmonary artery served as the reference region for the Logan plot analysis (28), which determined the distribution volume ratio (DVR) for ^{18}F-NOS. The supplemental materials provide details.

Metabolite Analysis

Metabolite analysis was performed on 5 of the 7 volunteers with evaluable data using high-performance liquid chromatography (HPLC). Eighteen total HPLC fractions were counted. The available parent compound in the plasma was then expressed as a percentage of the total activity. The supplemental materials provide details.

Statistical Analysis

A 2-way repeated-measures ANOVA tested for differences in DVR and mean HUs before and after endotoxin instillation in both the right and the left lungs using Sigmaplot 12.5.

(Systat Software, Inc.). The paired Student *t* test assessed for differences in the clinical parameters (vital signs, blood work, and pulmonary function tests) before and after endotoxin, with Bonferroni adjustments applied for multiple comparisons. When more than 1 measurement of any clinical parameter was obtained after endotoxin instillation, the most abnormal values or the values obtained immediately after PET imaging was completed were used for statistical testing.

RESULTS

Participant Flow and Clinical Characteristics

Nineteen healthy volunteers enrolled in the study. Eleven volunteers either failed screening procedures ($n = 10$) or withdrew consent ($n = 1$), leaving 8 who completed all study procedures. Of these 8, 1 volunteer had significant motion during the baseline PET/CT scan that could not be corrected, leaving a total of 7 volunteers with fully evaluable imaging data. Table 1 summarizes the demographics and clinical characteristics of these 7 volunteers. There were expected statistically significant increases after endotoxin in the total white blood cell count and peripheral blood neutrophil percentages. Statistically significant, but clinically in-significant, changes in temperature, heart rate, mean arterial pressure, and respiratory rate were also noted. As in our prior studies, no clinically significant adverse effects were noted after endotoxin instillation.

Endotoxin Increases iNOS Expression in BAL Cells But Not Exhaled Nitric Oxide Production

The mean BAL return volume from the endotoxin-challenged segment in the right middle lobe was 85 ± 9 mL. The total number of recovered cells (894 ± 431 cells/mm^3) and percentage of neutrophils (59% ± 12%) were within the expected range for this model (29). Immunohistochemical assessment of cells recovered by BAL demonstrated low-level iNOS expression in neutrophils and more intense iNOS expression in macrophages (Fig. 2). In 1 volunteer, little iNOS protein was detected in any cells with either antibody. The BAL cell counts and differentials (958 cells/mm^3, 55% neutrophils) as well as the return volume (90 mL) from this volunteer were not different from rest of the group. No differences in FeNO measurements were noted as a result of the endotoxin (26 ± 20 ppb before vs. 25 ± 16 ppb after endotoxin).

^{18}F-NOS Uptake Increases with iNOS Expression by Immunohistochemical Staining

^{18}F-NOS DVR was higher on the endotoxin-challenged side in the region of the infiltrate on CT. Figures 3 and 4 show representative images and time–activity curves, respectively. The average VOI size in the left lung was smaller (26 ± 8 mL on the left vs. 31 ± 10 mL on the right) because of the heart. All volunteers with positive iNOS staining had increased ^{18}F-NOS DVR accompanied by increased HUs on CT (Fig. 5). The 1 volunteer with low-level iNOS staining had no change in DVR despite an increased mean HU in the right lung infiltrate, the CT volume of which was also smaller, compared with other volunteers (4.5 mL).

^{18}F-NOS Blood Clearance Is Rapid

Approximately 40% of the parent compound was detected in the plasma at 15 min with approximately 17% remaining at 60 min after tracer injection (Fig. 6). Only 1 major metabolite eluted early from the HPLC column, indicating that this was a polar metabolite. The second peak of activity noted at approximately 10 min after tracer injection in the time–activity curves from both the venous blood samples and the pulmonary artery VOI (Supplemental Fig. 1) most likely represents the appearance of this metabolite.

DISCUSSION

Our findings suggest that ^{18}F-NOS uptake may reflect lung iNOS expression induced by bronchoscopically instilled endotoxin in healthy volunteers. The ^{18}F-NOS affinity for iNOS is 5-fold higher than endothelial NOS and 2-fold higher than neuronal NOS (22). In this study, we demonstrated that ^{18}F-NOS increased in all subjects who had detectable iNOS staining by immunohistochemistry. This increased ^{18}F-NOS uptake also correlated with evidence of inflammation by CT and BAL. In 1 volunteer with low-level iNOS expression by immunohistochemistry in cells from BAL, no increase in ^{18}F-NOS uptake was noted despite the presence of an infiltrate on CT and increased airway cell recruitment by BAL. These data therefore suggest that ^{18}F-NOS uptake in the lungs depends on iNOS expression.

The degree of ^{18}F-NOS uptake after endotoxin instillation was modest when compared with the higher ^{18}F-FDG uptake observed in the same model (24,25). Characteristics of the tracer itself may have contributed to this modest signal. Because this tracer is a reversible inhibitor of iNOS, no known trapping mechanism for signal amplification exists as for ^{18}F-FDG. Additionally, only approximately 50% of the parent compound was available for binding at 5 min after injection, with buildup of a single polar metabolite in the blood. Because of its polarity, this metabolite is most likely excluded by the lung endothelium from entering the lung parenchyma. Although the metabolite could certainly have leaked out of the vasculature as a result of the endotoxin-induced inflammation, our data suggest that this does not fully explain the uptake seen after endotoxin. The fact that we observed no change in DVR in 1 volunteer despite a clear infiltrate on CT indicates that simple vascular leak of either the parent compound or the metabolite is not enough to generate a signal with this tracer. Future studies that include measurements of extravascular lung water to compare the degree of vascular leak to ^{18}F-NOS uptake would help confirm these initial findings.

The modest ^{18}F-NOS signal may also have been due to characteristics of the model itself. The endotoxin induces early increases in cytokine and chemokine expression at 6 h, with continued neutrophil recruitment up to 24 h after instillation in healthy volunteers (29). In the present study, both the total cell numbers and the neutrophil percentages in the BAL increased when compared with previously reported numbers from saline-lavaged, normal control lung segments (29). Normal alveolar macrophages also express iNOS (11); thus, the higher level of staining noted in the macrophages compared with the neutrophils may not have changed significantly as a result of the endotoxin challenge. The modest ^{18}F-NOS signal may therefore have been primarily due to the recruitment of neutrophils with low-level iNOS staining. Additionally, iNOS expression in rodent models of lung inflammation peaks early, approximately 6–12 h after endotoxin administration (30). Although human

lung epithelium is also known to have substantial iNOS expression at baseline (11), the time course for epithelial iNOS upregulation after endotoxin in humans is unknown. Therefore, maximal epithelial iNOS expression may have occurred earlier as the peak expression of inflammatory cytokines has been demonstrated at 6 h after endotoxin in this model (29).

No change in ^{18}F-NOS uptake occurred in 1 volunteer with much lower iNOS immunohistochemical staining than in other volunteers. This volunteer, however, still had an infiltrate by CT and increased neutrophil recruitment by BAL after endotoxin instillation. Interestingly, the amount of infiltrate on CT, based on the VOI, was smaller than that of the other volunteers. Thus, the absence of iNOS staining may have indicated a functional defect in iNOS that limited the extent of the endotoxin-induced inflammation. Alternative splicing of iNOS messenger RNA and SNPs that could cause altered iNOS protein expression or function have been reported (31,32). However, we did not test for these variants. Instead, we tested for the TLR4 mutations Asp299Gly and Thr399Ile because they have been specifically associated with hyporesponsiveness to inhaled endotoxin (27). Interestingly, 1 volunteer who carried a single allele for each TLR4 SNP expressed iNOS (Fig. 5), whereas the volunteer with decreased iNOS expression did not carry any TLR4 SNPs (Fig. 5). Thus, the basis for decreased iNOS expression in this particular volunteer is unknown.

The overlap in absolute DVR values for ^{18}F-NOS measured before and after endotoxin may limit its clinical applicability. However, the absence of FeNO changes despite increased ^{18}F-NOS uptake suggests that this approach can detect mild segmental lung inflammation that is not great enough to change a global lung measurement such as the FeNO. Additionally, the dynamic range of this tracer may be higher in lung disease because the epithelium and BAL cells in asthma (14), chronic obstructive pulmonary disease (15), acute respiratory distress syndrome (18), postlung transplant bronchiolitis obliterans (33), and idiopathic pulmonary fibrosis (34) demonstrate higher iNOS expression than in healthy volunteers. This tracer may also still provide useful information about iNOS expression in clinical trials in which a baseline scan can be obtained before an antiinflammatory therapy is initiated. Nevertheless, 1 previously published study investigating ^{18}F-NOS in transplanted heart grafts demonstrated a small increase in signal, suggesting that further chemical modifications may be needed to improve in vivo binding (23). Such tracers could potentially image a wider range of in vivo iNOS expression in the lungs as well as other organ systems. Improvements would also potentially enable static image acquisitions to facilitate the clinical use of this approach.

CONCLUSION

We have demonstrated that ^{18}F-NOS is a potentially useful bio-marker of iNOS expression in the lungs. Used in conjunction with CT, this tracer may provide specific information about iNOS expression that can distinguish areas of lung parenchyma with active inflammation from areas affected by noninflammatory processes. Further studies to assess the dynamic range of this tracer in lung disease will help define its potential application as an inflammation-specific biomarker.

Supplementary Material

Refer to Web version on PubMed Central for supplementary material.

Acknowledgments

We thank Jinda Fan, Aixiao Li, and Lynne Jones for help with the metabolite analysis; Elizabeth Arentson for sample processing; Tamara Millay for study coordination and scheduling; Sharon Phillips for data organization and reporting; Tammy Koch and Brenda Patterson for pulmonary function testing; Linda Becker, Michael Harrod, and Betsy Thomas of the Center for Clinical Imaging Research for image acquisition and blood sample collection; the staff of the Washington University Cyclotron Facility for radiopharmaceutical production; and the Recruitment Enhancement Core staff of the Washington University Institute of Clinical and Translational Sciences for volunteer recruitment.

References

1. Murphy, SL.; Xu, JQ.; Kochanek, KD. National Vital Statistics Reports. Vol. 61. Hyattsville, MD: National Center for Health Statistics; 2013. Deaths: final data for 2010.
2. Mathers CD, Loncar D. Projections of global mortality and burden of disease from 2002 to 2030. PLoS Med. 2006; 3:e442. [PubMed: 17132052]
3. Walkey AJ, Summer R, Ho V, Alkana P. Acute respiratory distress syndrome: epidemiology and management approaches. Clin Epidemiol. 2012; 4:159–169. [PubMed: 22866017]
4. Adams CP, Brantner VV. Estimating the cost of new drug development: is it really 802 million dollars? Health Aff (Millwood). 2006; 25:420–428. [PubMed: 16522582]
5. Martinez FJ, Donohue JF, Rennard SI. The future of chronic obstructive pulmonary disease treatment: difficulties of and barriers to drug development. Lancet. 2011; 378:1027–1037. [PubMed: 21907866]
6. Self WH, Courtney DM, McNaughton CD, Wunderink RG, Kline JA. High discordance of chest x-ray and computed tomography for detection of pulmonary opacities in ED patients: implications for diagnosing pneumonia. Am J Emerg Med. 2013; 31:401–405. [PubMed: 23083885]
7. Bellani G, Messa C, Guerra L, et al. Lungs of patients with acute respiratory distress syndrome show diffuse inflammation in normally aerated regions: a [^{18}F]-fluoro-2-deoxy-D-glucose PET/CT study. Crit Care Med. 2009; 37:2216–2222. [PubMed: 19487931]
8. Chen DL, Ferkol TW, Mintun MA, Pittman JE, Rosenbluth DB, Schuster DP. Quantifying pulmonary inflammation in cystic fibrosis with positron emission tomography. Am J Respir Crit Care Med. 2006; 173:1363–1369. [PubMed: 16543553]
9. Jones HA, Marino PS, Shakur BH, Morrell NW. In vivo assessment of lung inflammatory cell activity in patients with COPD and asthma. Eur Respir J. 2003; 21:567–573. [PubMed: 12762337]
10. Subramanian D, Jenkins L, Edgar R, Quraishi N, Stockley R, Parr D. Assessment of pulmonary neutrophilic inflammation in emphysema by quantitative positron emission tomography. Am J Respir Crit Care Med. 2012; 186:1125–1132. [PubMed: 22837375]
11. Guo FH, De Raeve HR, Rice TW, Stuehr DJ, Thunnissen FB, Erzurum SC. Continuous nitric oxide synthesis by inducible nitric oxide synthase in normal human airway epithelium in vivo. Proc Natl Acad Sci USA. 1995; 92:7809–7813. [PubMed: 7544004]
12. Stuehr DJ. Mammalian nitric oxide synthases. Biochim Biophys Acta. 1999; 1411:217–230. [PubMed: 10320659]
13. Ricciardolo FL, Timmers MC, Geppetti P, et al. Allergen-induced impairment of bronchoprotective nitric oxide synthesis in asthma. J Allergy Clin Immunol. 2001; 108:198–204. [PubMed: 11496234]
14. Redington AE, Meng QH, Springall DR, et al. Increased expression of inducible nitric oxide synthase and cyclo-oxygenase-2 in the airway epithelium of asthmatic subjects and regulation by corticosteroid treatment. Thorax. 2001; 56:351–357. [PubMed: 11312402]
15. Ichinose M, Sugiura H, Yamagata S, Koarai A, Shirato K. Increase in reactive nitrogen species production in chronic obstructive pulmonary disease airways. Am J Respir Crit Care Med. 2000; 162:701–706. [PubMed: 10934109]

16. Maestrelli P, Paska C, Saetta M, et al. Decreased haem oxygenase-1 and increased inducible nitric oxide synthase in the lung of severe COPD patients. Eur Respir J. 2003; 21:971–976. [PubMed: 12797490]
17. Ricciardolo FL, Caramori G, Ito K, et al. Nitrosative stress in the bronchial mucosa of severe chronic obstructive pulmonary disease. J Allergy Clin Immunol. 2005; 116:1028–1035. [PubMed: 16275371]
18. Sittipunt C, Steinberg KP, Ruzinski JT, et al. Nitric oxide and nitrotyrosine in the lungs of patients with acute respiratory distress syndrome. Am J Respir Crit Care Med. 2001; 163:503–510. [PubMed: 11179131]
19. Kobayashi A, Hashimoto S, Kooguchi K, et al. Expression of inducible nitric oxide synthase and inflammatory cytokines in alveolar macrophages of ARDS following sepsis. Chest. 1998; 113:1632–1639. [PubMed: 9631804]
20. Seimetz M, Parajuli N, Pichl A, et al. Inducible NOS inhibition reverses tobacco-smoke-induced emphysema and pulmonary hypertension in mice. Cell. 2011; 147:293–305. [PubMed: 22000010]
21. Bhandari V, Choo-Wing R, Chapoval SP, et al. Essential role of nitric oxide in VEGF-induced, asthma-like angiogenic, inflammatory, mucus, and physiologic responses in the lung. Proc Natl Acad Sci USA. 2006; 103:11021–11026. [PubMed: 16832062]
22. Zhou D, Lee H, Rothfuss JM, et al. Design and synthesis of 2-amino-4-methylpyridine analogues as inhibitors for inducible nitric oxide synthase and in vivo evaluation of [^{18}F]6-(2-fluoropropyl)-4-methyl-pyridin-2-amine as a potential PET tracer for inducible nitric oxide synthase. J Med Chem. 2009; 52:2443–2453. [PubMed: 19323559]
23. Herrero P, Laforest R, Shoghi K, et al. Feasibility and dosimetry studies for ^{18}F-NOS as a potential PET radiopharmaceutical for inducible nitric oxide synthase in humans. J Nucl Med. 2012; 53:994–1001. [PubMed: 22582045]
24. Chen DL, Rosenbluth DB, Mintun MA, Schuster DP. FDG-PET imaging of pulmonary inflammation in healthy volunteers after airway instillation of endotoxin. J Appl Physiol. 2006; 100:1602–1609. [PubMed: 16424067]
25. Chen DL, Bedient TJ, Kozlowski J, et al. [^{18}F]fluorodeoxyglucose positron emission tomography for lung antiinflammatory response evaluation. Am J Respir Crit Care Med. 2009; 180:533–539. [PubMed: 19574441]
26. Dweik RA, Sorkness RL, Wenzel S, et al. Use of exhaled nitric oxide measurement to identify a reactive, at-risk phenotype among patients with asthma. Am J Respir Crit Care Med. 2010; 181:1033–1041. [PubMed: 20133930]
27. Arbour NC, Lorenz E, Schutte BC, et al. TLR4 mutations are associated with endotoxin hyporesponsiveness in humans. Nat Genet. 2000; 25:187–191. [PubMed: 10835634]
28. Logan J, Fowler JS, Volkow ND, Wang GJ, Ding YS, Alexoff DL. Distribution volume ratios without blood sampling from graphical analysis of PET data. J Cereb Blood Flow Metab. 1996; 16:834–840. [PubMed: 8784228]
29. O'Grady NP, Preas HL, Pugin J, et al. Local inflammatory responses following bronchial endotoxin instillation in humans. Am J Respir Crit Care Med. 2001; 163:1591–1598. [PubMed: 11401879]
30. Kristof AS, Goldberg P, Laubach V, Hussain SN. Role of inducible nitric oxide synthase in endotoxin-induced acute lung injury. Am J Respir Crit Care Med. 1998; 158:1883–1889. [PubMed: 9847282]
31. Eissa NT, Strauss AJ, Haggerty CM, Choo EK, Chu SC, Moss J. Alternative splicing of human inducible nitric-oxide synthase mRNA: tissue-specific regulation and induction by cytokines. J Biol Chem. 1996; 271:27184–27187. [PubMed: 8900212]
32. Qidwai T, Jamal F. Inducible nitric oxide synthase (iNOS) gene polymorphism and disease prevalence. Scand J Immunol. 2010; 72:375–387. [PubMed: 21039732]
33. Gabbay E, Walters EH, Orsida B, et al. Post-lung transplant bronchiolitis obliterans syndrome (BOS) is characterized by increased exhaled nitric oxide levels and epithelial inducible nitric oxide synthase. Am J Respir Crit Care Med. 2000; 162:2182–2187. [PubMed: 11112135]

34. Saleh D, Barnes PJ, Giaid A. Increased production of the potent oxidant peroxynitrite in the lungs of patients with idiopathic pulmonary fibrosis. Am J Respir Crit Care Med. 1997; 155:1763–1769. [PubMed: 9154889]

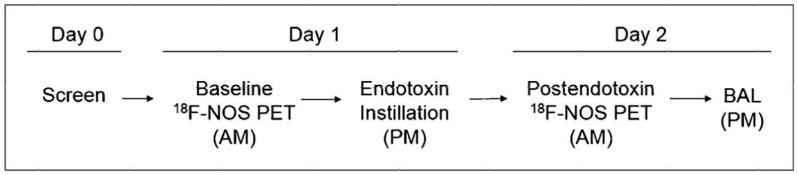

FIGURE 1.

Study design. Postendotoxin ^{18}F-NOS PET scan occurred at approximately 16 h after endotoxin instillation.

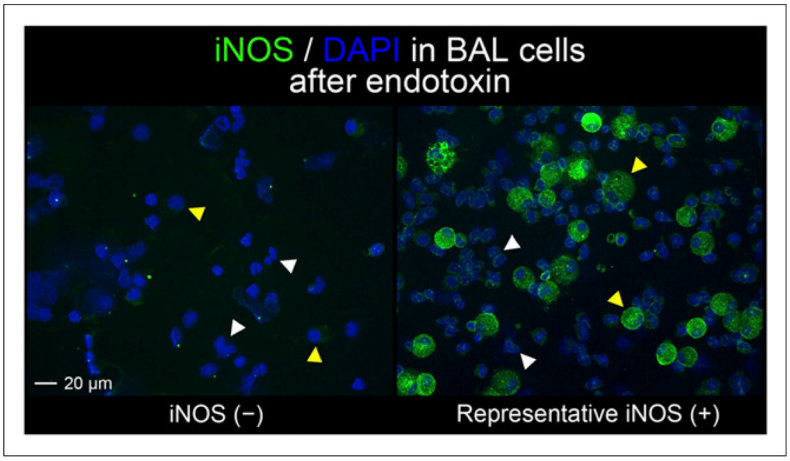

FIGURE 2.

Immunohistochemical staining for iNOS (green) in cells obtained by BAL in endotoxin-challenged airway. Only 1 individual had negative iNOS staining (iNOS (−)). iNOS (+) image is representative of positive staining results obtained on BAL cells from 6 volunteers. Neutrophils (white arrowheads) and macrophages (yellow arrowheads) were identified by nuclear morphology from 4′,6-diamidino-2-phenylindole staining (blue). Images taken at ×20 magnification.

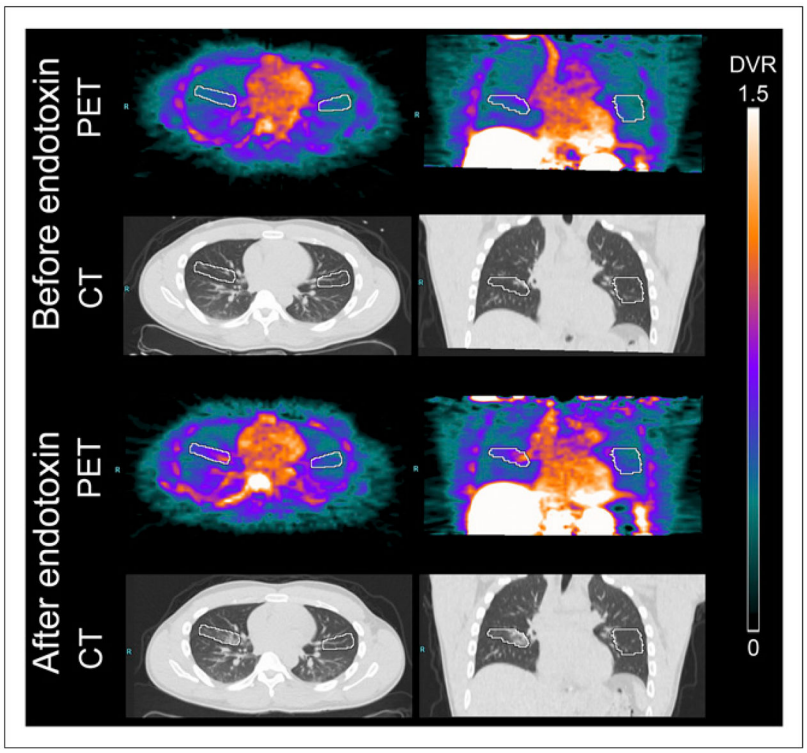

FIGURE 3.

Representative Logan parametric ^{18}F-NOS PET/CT images (DVR scale, mL lung/mL blood) obtained before and after bronchoscopic instillation of endotoxin in right middle lobe. VOIs are shown in white.

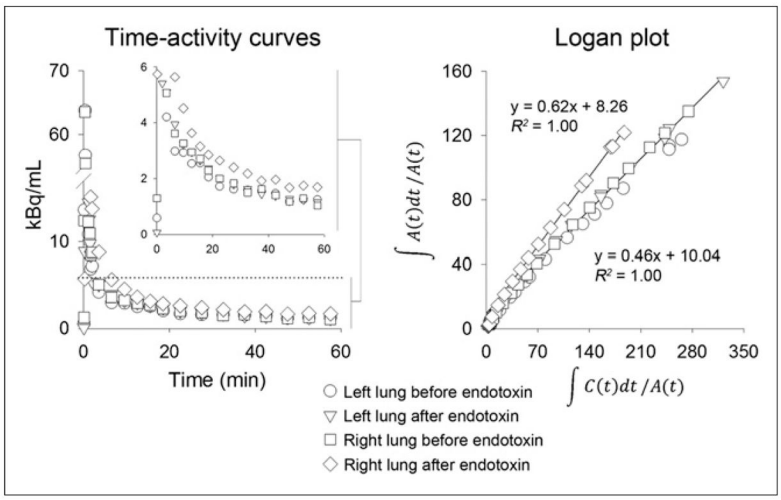

FIGURE 4.

Time–activity curves and Logan plots from images (VOI) in Figure 3. Last 12 data points (last 50 min of image acquisition) were used for Logan plot linear regression for all scans. Inset shows later time points of curve focused on lower range activity to better illustrate differences in activity among different VOIs. Units for Logan plot axes: *x*-axis = mL blood/mL lung × min; *y*-axis = min.

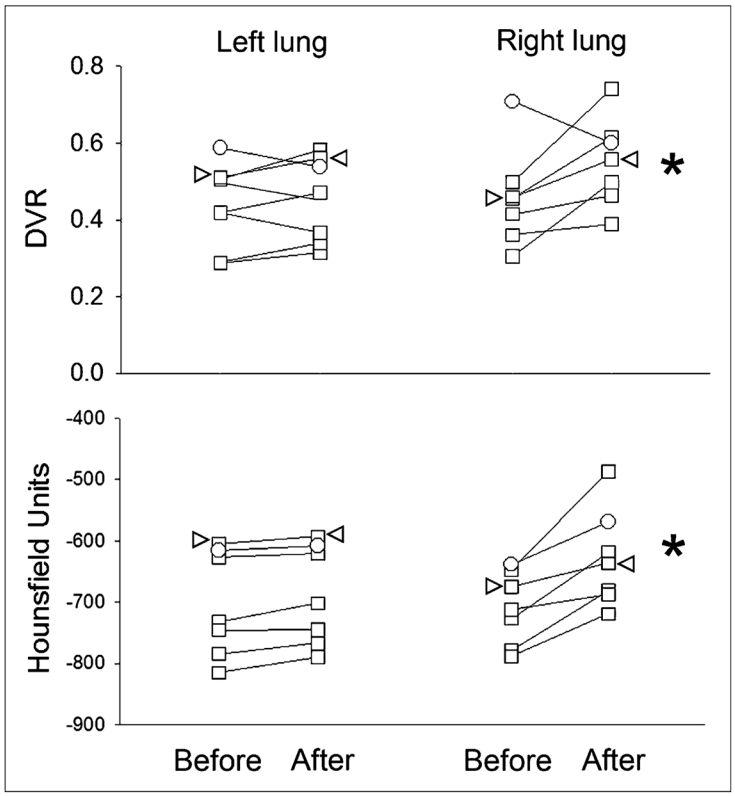

FIGURE 5.

^{18}F-NOS DVR and mean HUs in right and left lung VOIs before and after endotoxin instillation in right middle lobe. White circles denote 1 volunteer without iNOS in BAL cells. Arrowheads denote data from 1 volunteer with heterozygosity for 2 TLR4 single nucleotide polymorphisms reported to predict endotoxin hyporesponsiveness. *$P < 0.05$, compared with either left lung after endotoxin or right middle lobe before endotoxin. Before = before endotoxin instillation; After = 16 h after endotoxin instillation.

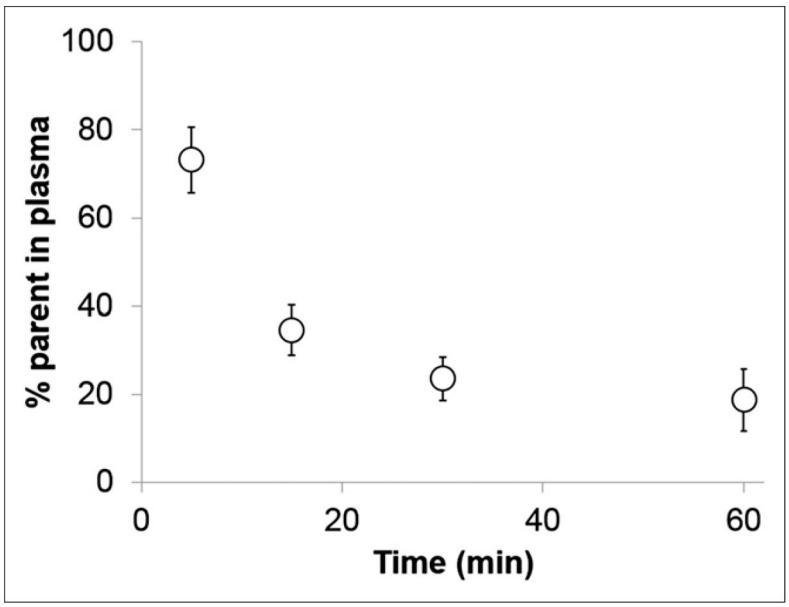

FIGURE 6.

^{18}F-NOS metabolism showing percentage of parent compound in plasma. Values are shown as mean ± SD bars.

TABLE 1

Summary Characteristics for All Volunteers Completing Study Procedures with Evaluable Data

Parameter	Before endotoxin	16 h after endotoxin	Most abnormal value after endotoxin	*P*
Age (y)	35 ± 6	N/A	N/A	N/A
Sex	3 women, 4 men	N/A	N/A	N/A
Race/ethnicity	3 Caucasian/4 African-American	N/A	N/A	N/A
Vital signs*				
Temperature (ºC)	36.5 ± 0.3	36.3 ± 0.4	37.3 ± 0.3 (highest)	0.0016†
Heart rate (beats/min)	69 ± 11	72 ± 11	92 ± 9 (highest)	0.0015†
			60 ± 6 (lowest)	0.0208
Blood pressure, systolic/diastolic (mm Hg)	116 ± 6/69 ± 5	113 ± 6/72 ± 5	100 ± 13/50 ± 6 (lowest)	0.0071/0.016
Mean arterial pressure	85 ± 5	85 ± 5	69 ± 7 (lowest)	0.0000†
S_aO_2 (% on room air)	99 ± 1	99 ± 1	95 ± 2 (lowest)	0.016
Respiratory rate (breaths/min)	17 ± 1	18 ± 2	22 ± 2 (highest)	0.0002†
Pulmonary function tests				
FEV_1 (L)	3.7 ± 0.7	3.6 ± 0.6	N/A	0.424
% predicted FEV_1	108 ± 12	106 ± 16	N/A	0.548
FVC (L)	4.5 ± 1.0	4.5 ± 0.9	N/A	0.824
% predicted FVC	108 ± 10	109 ± 15	N/A	0.888
Complete blood count				
White blood cells ($\times 10^3/\mu L$)	6.6 ± 1.4	10.8 ± 2.4†	N/A	0.0026†
% neutrophils	62 ± 5	73 ± 7†	N/A	0.0069
Hemoglobin (g/dL)	14 ± 2	13 ± 2	N/A	0.16
Hematocrit (%)	41 ± 5	38 ± 6	N/A	0.183
Platelets ($\times 10^3/\mu L$)	274 ± 59	254 ± 38	N/A	0.247
ESR (mm/h)	20 ± 18	18 ± 14	N/A	0.337
Change in ESR	N/A	-2.4 ± 6.2	N/A	
CRP (mg/dL)	9 ± 15	14 ± 19	N/A	0.016
Change in CRP	N/A	5.1 ± 3.6	N/A	

*Statistical testing for vital signs was performed only on the most abnormal value after endotoxin instillation.

†$P < 0.0026$ (significance level with Bonferroni adjustment).

N/A = not applicable; FEV_1 = forced expiratory volume in 1 s; FVC = forced vital capacity; ESR = erythrocyte sedimentation rate; CRP = C-reactive protein.